Int. J. Electrochem. Sci., 12 **(2017)** 8411 – 8420, doi: 10.20964/2017.09.09

International Journal of
ELECTROCHEMICAL
SCIENCE
www.electrochemsci.org

Short Communication

Fabrication of Biosensor for Selective Electrochemical Determination of Glycated Hemoglobin

Min Li[1], *Wenjie Zhao*[1], *Linlin Tian*[1], *Huafeng Li*[1] *and Bo Fan*[2,*]

[1] Department of Endocrinology, The Third Affiliated Hospital of Qiqihaer Medical University, 27 Taishun Road, Qiqihaer, Heilongjiang, 161000, P.R. China
[2] Department of Electrophysiology, The Third Affiliated Hospital of Qiqihaer Medical University, 27 Taishun Road, Qiqihaer, Heilongjiang, 161000, P.R. China
[*]E-mail: fanbo543@yeah.net

Received: 13 May 2017 / *Accepted:* 25 June 2017 / *Published:* 13 August 2017

The glucose level in diabetic patients should be detected without short-term fluctuations. Diabetes mellitus was used as a platform to investigate the glycated hemoglobin (HbA1c) level. HbA1c tops the list of main factors in discerning the concentration of the average plasma glucose during an extended period. In this study, a biosensor was fabricated based on a nitrogen-doped graphene/gold nanoparticle (AuNP)/fluorine-doped tin oxide (FTO) glass electrode immobilized with fructosyl amino-acid oxidase (FAO). This biosensor is highly sensitive and selective towards the determination of HbA1c. The limit of detection (LOD) is 1.70 μg/mL, and the linear range is 10-65 μg/mL.

Keywords: Glycated hemoglobin; Fructosyl amino-acid oxidase; Nitrogen-doped graphene; Electrochemical determination; AuNPs

1. INTRODUCTION

As a glycosylated hemoglobin, glycated hemoglobin (HbA1c) is formed through the non-enzymatic reaction of glucose with the N-terminal valine of the β-chain of normal adult hemoglobin (HbA0) [1-3]. The ratio between the concentration of HbA1c and total hemoglobin concentration is termed the level of HbA1c, which is viewed as a diagnostic biomarker for diabetic patients, in addition to the blood glucose level assay. The clinical reference range of HbA1c to total hemoglobin (HbA0) is 5%–20%, where 4%–6.5% is viewed as normal [4]. The blood glucose level of a diabetic is characteristically unstable, even within a one day period. Therefore, the HbA1c level assay could be desirably indicative of the blood glucose for 8-12 weeks. Hence, the HbA1c level assay is of vital importance to the long-term control of the glycemic state in diabetic patients [5].

Ion-exchange and boronated affinity chromatography [6, 7], electrophoresis [8] and fluorescence [9, 10] are conventional techniques of HbA1c detection. However, these techniques are comparatively high-cost and entail blood specimen pretreatment, a professional experimenter and a long detection time. Therefore, it is of clinical and scientific significance to propose a disposable and single-use in vitro biosensor to selectively and sensitively detect HbA1c for diabetes management. This biosensor is rapid in response time (on the level of one second) and could specifically and sensitively determine HbA1c in adequate physiological range. In addition, it requires only a small specimen volume (10–15 μL of blood or other physiological fluids). Therefore, the proposed HbA1c detection biosensor could not only function as an independent monitoring configuration but also be used to make up a double diagnosis configuration for simultaneous measurement of the HbA1c and blood glucose.

The surface of an electrode element is modified to increase the affiliation of the electrochemical biosensor towards HbA1c via sugar-binding materials (mainly boronic acid), proteins and antibodies specific to HbA1c. A transduction process, which includes voltammetry/amperometry, impedometry or potentiometry, then follows after the aforementioned bio-recognition process [10, 11]. Zhou and co-workers [12] proposed electrochemical BPA-PQQ/ERGO-based glassy carbon electrode (GCE) towards HbA1c detection with differential pulse voltammetry (DPV). However, the proposed electrode was in-disposable and the preparation entailed many different steps. In addition, the boronic acid derivative had affinity to a wide range of sugars and glycated proteins not exclusive to HbA1c; thus, the biosensor was not desirable for the detection of HbA1c. Chopra et al. [13] developed a sandwich-type electrochemical immunoassay technique based on a screen-printed gold electrode, where the capture molecule and tracer were MPBA-SAM and ferrocene labeled anti-HbA1c, respectively. Kim et al. [14] studied the catalytic feature of HbA1c for the reduction of H_2O_2 to assay the HbA1c level. The preparation of the sensor entailed several potential cycling steps and electrodeposition. In addition, this sensor employed aminophenyl boronic acid as the boronic acid–derivative capturing probe. Furthermore, it entailed a pretreatment step for the blood specimen to remove glucose and other glycated proteins. Electrochemical impedance spectroscopy (EIS) measurements, for the determination of HbA1c, were also studied [15, 16]. In comparison with voltammetry/amperometry routes, EIS entails complicated devices and a lengthened measurement time. After data collection, equivalent circuit modeling is another additional step for the EIS measurement.

In recent years, biocompatible nanomaterials have been proposed for the development of novel, direct biomolecule-electrode electron transfer based biosensors [17]. As an effective biocompatible 2D nanomaterial, graphene nanosheets (GNs) have been viewed as a novel material with potential application in relevant fields including the following: chemical processing, biosensors, and physics, such as bio electronics and classical electronics [18-20]. A carbon-based material could be effectively varied in intrinsic features, including their surface framework and electronics, to achieve an accurate modification. Subsequently, the aforementioned metal nanoparticles are designed to introduce interlayers of GNs to GNs-based nanomaterials, which prevent their aggregation. Hence, a useful chemical approach for the direct and uniform attachment of gold nanoparticles (AuNPs) with high

density GNs was realized to form an immobilization platform for the protein ascribed to the strong binding between the GNs and metal nanoparticles [21].

This study proposed the fabrication of the N-doped GNs with AuNPs using an ethylene glycol reduction method. The biosensor was further employed to detect HbA1c. UV–vis analysis, X-ray diffraction and spectrophotometry were performed for different measurements. The cyclic voltammetry (CV) and electrochemical impedance spectroscopy (EIS) measurements were carried out after enzyme immobilization. The AuNPs/GNs composite film could selectively detect HbA1c in human blood specimens because of its effective electrochemical response.

2. EXPERIMENTS

2.1. Chemicals

Chitosan, urea, 4-aminoantipyrine, graphite, proteases, $HAuCl_4$, ethylene glycol (EG), MES (4-Morpholinoethane sulfonic acid), pyridine, Dess-Martin periodinane and L-valine were commercially available from Sigma Chemical Co. The fluorine-doped tin oxide (FTO) glass electrode, glutaraldehyde (GA), bovine serum albumin (BSA) and fructosyl-amino acid oxidase (FAO) were commercially available from Sigma Aldrich. Distilled water (DW) was used throughout. Fresh, whole blood specimens from healthy persons and diabetic individuals were obtained from The Third Affiliated Hospital of Qiqihar and stored at 4 °C before use.

2.2. Preparation of the N-doped graphene nanosheets (GNs)

Concentrated sulfuric acid (50 mL) was added to graphite (2.0 g) in a conical flask (250 mL) at 25 °C and vigorously stirred to yield graphene. This process was followed by careful and slow pouring of $NaNO_2$ (2.0 g) and $KMnO_4$ (6.0 g) into the obtained mixture, which was then gently mixed. Next, a heat treatment for 20 h at 25 °C, DW (80 mL) was introduced dropwise into this mixture, which was then left to stand for 15 min. This process was followed by pouring H_2O_2 (20 mL, 30%) into the as-prepared mixture. The obtained mixture was exposed to a hydrochloric acid solution, washing once, and to DW, washing three times. To yield a 5 mg/mL aqueous dispersion of graphene, the precipitate from the above treatment was ultra-sonicated and suspended in DW. Graphene, with a high N-content, was prepared using a one-pot route, with a chemical dopant of urea [22]. This process was followed by dispersing GNs (10 mL, 50 mg) into DW (25 mL). The GNs dispersion was then added to urea (2 g) and sonicated for 4 h. The as-prepared solution was introduced into a Teflon-lined autoclave (50 mL) and stored at 150 °C for 5 h. The solids (N-doped GNs) were filtered and washed with DW 3 times. Finally, after the as-prepared specimen was left to dry in a vacuum oven, the N-doped GNs were obtained.

2.3. Preparation of N-doped GNs embedded AuNPs (AuNPs/GNs)

GNs and gold-precursor salts were collectively added to the EG solution to validate the functionalization of the AuNPs on the N-doped GNs [23]. Briefly, after the introduction of N-doped

GNs (50 mg) to the aqueous solution (50 mL) and 0.02 mM $HAuCl_4$, the obtained mixture was exposed to ultrasonication for 120 min to yield to stable colloid, which was injected with EG (20 mL) and continuously mixed for 120 min. The resulting mixture was kept at 130 °C for 6 h under continuous agitation, filtered, and washed using DW to yield the AuNPs/N-GN composite.

2.4. Enzyme immobilization

The FTO electrode was completely cleaned, first using acetone under an ultrasonic bath for 10 min and then using DW for another 10 min. The AuNPs/N-GNs were electrochemically deposited on 3 electrodes, when merged in the electrochemical cell at −0.6 V using chronoamperometry at the reference electrode. The counter and working electrodes were Pt wire and FTO electrodes (area of 1 cm^2), respectively. After drying at ambient temperature, a freshly coated film was employed. The enzyme concentrations at 5, 15, 25, and 35 IU were measured to optimize the enzyme concentration.

Chitosan was dissolved in acetic acid (1% *v/v*) under ultrasonication for 60 min and vortexed to yield a 1% (*w*/*v*) chitosan solution. The FTO electrode dropped with 4 μL of the chitosan solution was dried at 30 °C for 12 h. BSA (4%) and FAO (1%) were used to prepare the enzyme solution to fabricate the biosensors, where every 100 μL of enzyme solution contained 25 U FAO. The obtained enzyme solution had an additional 2.5% GA solution added with a ratio of 2:1 FAO solution: GA. Subsequently, 2 μL of the mixed solution was spread onto the FTO electrode and dried at 4 °C for 4 h. The modified electrode was denoted by AuNPs/N-doped GNs/FTO.

2.5. Characterization

A UV-Vis spectrophotometer (Halo RB-10, Dynamica Pty Ltd, AU) and X-ray diffractometer (D8 –Advance XRD, Bruker, Germany) with Cu Kα radiation were used to obtain the optical information and crystal characterization of the nanocomposite, respectively. A CH Instruments 660A electrochemical Workstation (CHI-660 A, CH Instruments, Texas, USA) consisting of a triple-electrode configuration was used for electrochemical assays. The reference and auxiliary electrodes were Ag/AgCl (3M KCl) and a platinum wire, respectively. The electron transfer behavior on the surface of the bare and modified electrode was characterized via electrochemical impedance spectroscopy (EIS). The supporting electrolyte and probe were KCl (0.1 M) and $[Fe(CN)_6]^{3-/4-}$ (5 mM). The amplitude was 5 mV, and the frequency ranged from 10^1 to 10^5 Hz. With regard to DPV determination, the scan range was -0.6 to -0.4 V with a scan rate of 0.5 mV/s, while the modulation took 0.05 s with an interval of 0.2 s.

3. RESULTS AND DISCUSSION

An obvious XRD peak of 2 theta at 13.4 degrees was viewed as a standard for graphene oxide and was the focus of the study. A peak shift to the right and formation of a wide peak were observed after an additional heat treatment and nitrogen involved doping, suggesting graphene oxide (GO) was

reduced into graphene, as indicated in Figure 1A. The diffraction peaks from numerous planes and d-values accurately matched JCPDS reported data for GNs [24]. The relative peak intensities and positions of GNs were arranged based on standard JCPDS, without the observation of impurities. The UV–vis spectrum showed a π–π* transition of GO at 228 nm. An absorption peak at 307 nm is due to the n-π* transition of the C–O bonds and embedded via the inclusion and exfoliation on the graphene. The reduction of the GO to graphene was analyzed using N-doping, where the 275 nm peak was observed. As indicated in Figure 1B, the AuNPs contributed to the additional peak observed at 535 nm.

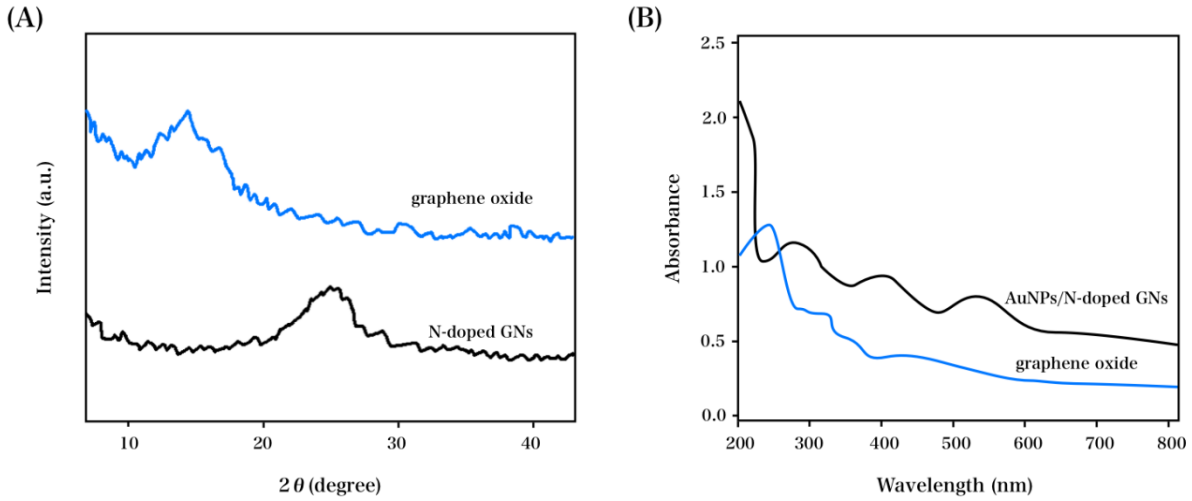

Figure 1. (A) X-ray diffraction (XRD) profile of graphene oxide and N-doped GNs. (B) Absorption characterizations of graphene oxide and AuNPs/N-doped GNs in aqueous solution.

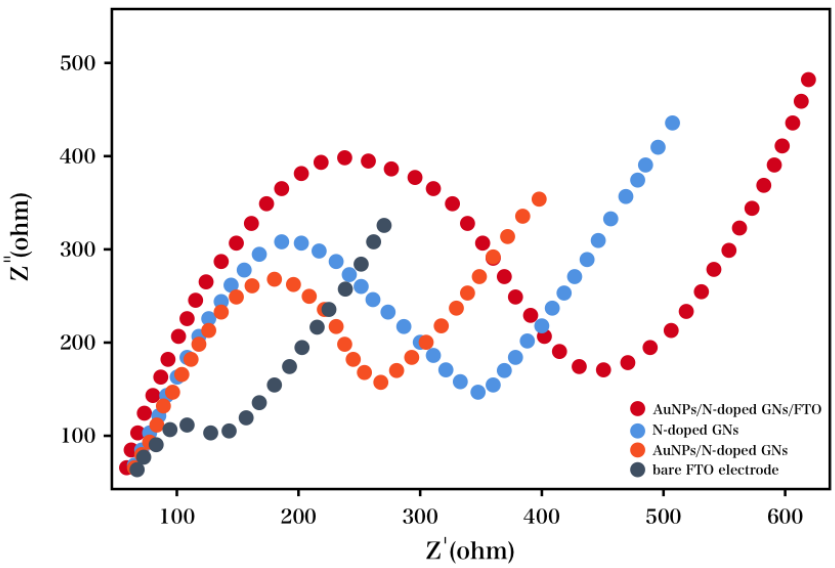

Figure 2. EIS Nyquist plots of the original FTO electrode, N-doped GNs, AuNPs/N-doped GNs and AuNPs/N-doped GNs/FTO in 0.1 M KCl + 5 mM $[Fe(CN)_6]^{3/4}$. The frequency range: 0.1 Hz - 100 kHz; amplitude of sine voltage signal: 5 mV.

EIS has been recognized as a facile route to study the stepwise modification process, where the electrode exhibited interface feature variations. Experiments were carried out in a 0.1 M KCl solution with 5 mM $Fe(CN)_6^{4-/3-}$ as the redox probe, and the frequency range used was between 0.1 Hz and 10^5 Hz, with a signal amplitude of 5 mV. As shown in Figure 2, the diameter of the semicircle calculated from the Nyquist plot corresponds to the electron transfer resistance (R_{ct}) [25]. The original FTO electrode showed the electron transfer resistance (R_{ct}) as 1007 Ω. With respect to GNs and AuNPs/GNs/FTO electrodes, the R_{ct} value declined to 221 Ω and 114 Ω, respectively (Figure 3), indicating that nanocomposites between the electrode surface and electrolyte showed rapid electron exchange kinetics. The obtained results were consistent with that expectation, confirming the positive effect of the as-prepared AuNPs/GNs composite on the improvement of interfacial electron transfer [26]. As shown in Curve d, there was an increase in the R_{ct} value up to 448 Ω, observed on the FAO/AuNPs/GNs/FTO electrode, since the FAO molecules formed a barrier layer and led to the hindrance of the electron exchange channel via the enzyme.

The DPV curves obtained at the AuNPs/N-doped GNs/FTO, in the presence and absence of HbA_{1c} in the phosphate buffer solution (PBS) (0.1 M, pH 8.0), were compared in Figure 3. In the presence of HbA_{1c}, AuNPs/N-doped GNs/FTO showed a pronounced decline in the oxidation peak current, due to the hindrance of the electron exchange by the protein molecules. The results suggested the binding of HbA_{1c} onto the surface of the electrode and the usability of the electrochemical measurement for the determination of HbA_{1c}. With respect to control groups, extremely small current responses were observed for HbA_{1c} on the original FTO and N-doped GNs/FTO before and after the addition of HbA_{1c}. These could be attributed to the low loading of HbA_{1c} on the bare FTO and N-doped GNs/FTO electrodes, demonstrating that the N-doped GNs played a key role for electro-catalytic determination.

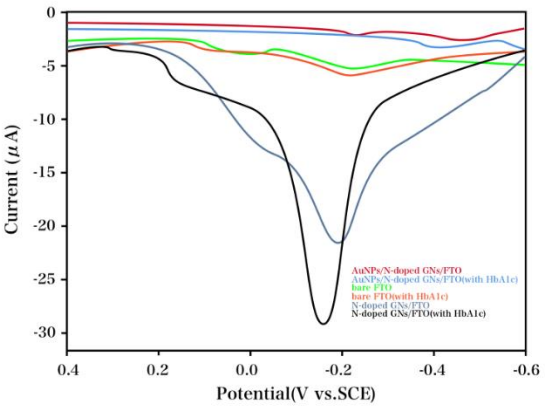

Figure 3. DPV characterization of the AuNPs/N-doped GNs/FTO, the original FTO and N-doped GNs/FTO in phosphate buffer (0.1 M, pH 8.0) before and after adding HbA_{1c} solution (50 μg/mL).

Certain factors, including the pH of the buffer, incubation temperature, and incubation time, were found to play important roles in the binding of HbA_{1c} to the electrochemical sensor [14, 27, 28]. The binding of HbA_{1c} to the electrode could be affected by the pH value, causing variation in the

current response of the sensor. Therefore, the determination behavior depended on the pH value. As indicated in Figure 4A, a pH value ranging from 5 to 9 was used to investigate the effect of the pH value on the current response toward HbA_{1c} determination. With the increase in pH in the range of 5 to 8, there was a gradual increase in the I_d value. With further increase in the pH value (over 8), a decrease in I_d value was observed. Therefore, the pH value was optimized as 8, where the maximal I_d value was obtained, which is in accordance with the findings that the binding of boronic acid with the diol of HbA_{1c} occurred under weak alkaline conditions [29]. The pH value of 8 for the buffer solution was selected. The effect of incubation time on the response was investigated in Figure 4B. As the incubation time increased, there was an increase in the I_d value, reaching a plateau after 0.5 h. Hence, the optimum incubation time was selected as 0.5 h. The effect of incubation temperature on the current response was indicated in Figure 4C. As the temperature increased within the range of 5 - 30 °C, a slight increase in the I_d value was observed. The I_d value dropped because of the thermal deactivation of HbA_{1c}. Therefore, 30 °C was set as the optimum incubation temperature.

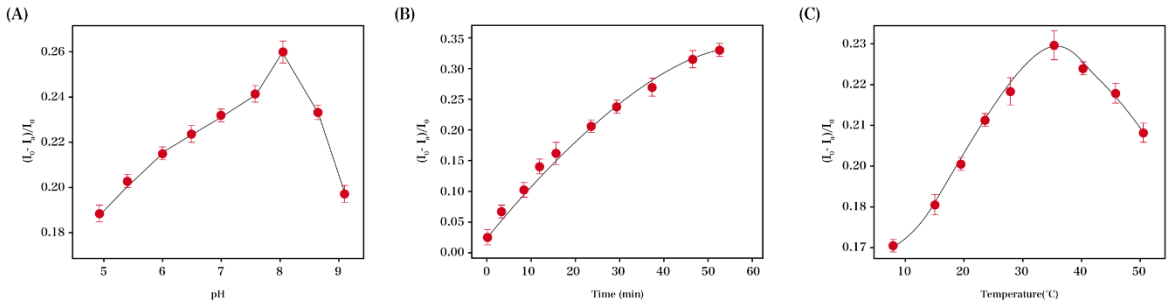

Figure 4. Optimization of experimental parameters for the determination of HbA_{1c} at the AuNPs/N-doped GNs/FTO: (A) Effect of pH value on phosphate buffer (0.1 M); (B) Effect of reaction time on phosphate buffer (0.1 M, pH 8.0); (C) Effect of reaction temperature on phosphate buffer (0.1 M, pH 8.0).

To quantitatively detect HbA_{1c}, DPV curves of the AuNPs/N-doped GNs/FTO, after the addition of varied concentrations of HbA_{1c}, was studied under optimum conditions. With the increase in HbA_{1c} concentration, a decrease in the oxidation peak current was observed (Figure 5A); the I_d value was in a linear relationship with the HbA_{1c} concentration, ranging from 10 to 65 μg/mL (Figure 5B). Since the active sites decreased on the surface of the electrode used for target binding, there was a curvature when at a high concentration, with a limit of detection (LOD) of 1.70 μg/mL (S/N=3). The proposed sensor is comparable in sensitivity to other traditional electrochemical techniques. Due to the physiological HbA_{1c} level range of 3 - 13 mg/mL in human blood specimens, the proposed technique could adequately detect the HbA_{1c} in real blood specimens after the dilution using the buffer solution.

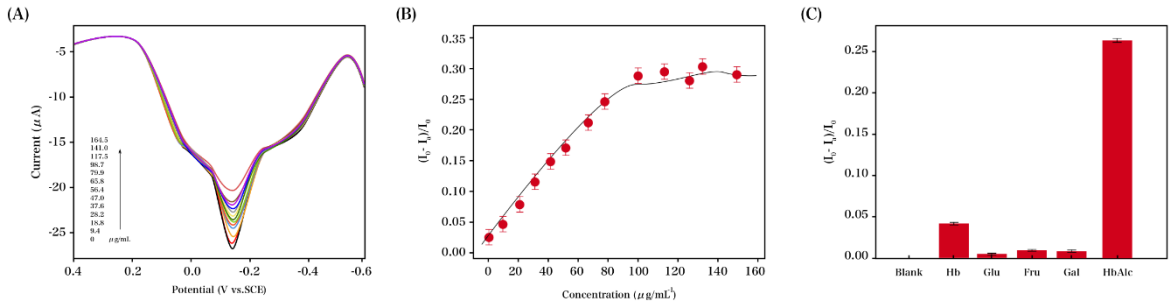

Figure 5. (A) DPV profiles of an increasing concentration of HbA_{1c} in the phosphate buffer (0.1 M, pH 8.0) at the AuNPs/N-doped GNs/FTO. (B) Linear calibration plot of I_d value *versus* the concentration of HbA_{1c}. (D) Selectivity of the AuNPs/N-doped GNs/FTO towards the target HbA_{1c} in comparison with galactose, fructose, glucose and Hb in phosphate buffer (0.1 M, pH 8.0).

Other interferents were also analyzed under the same conditions to assess the selectivity of our proposed electrochemical determination of HbA_{1c}. The HbA_{1c} was compared with interferents such as galactose, fructose, glucose and Hb, and their corresponding electrochemical responses are shown in Figure 5C. The statistical data have been summarized in Table 2. Since the electrochemical response was not affected by the binding of small molecules on the electrode surface, these small molecules did not influence the determination of HbA_{1c}. Since Hb adsorbed onto the surface of the electrode, the I_d value showed a slight increase after the addition of Hb, although it was negligible. Therefore, the highly selective technique was successful in detecting HbA_{1c} in biological specimens.

Table 1. Comparison of analytical characteristics for the determination of HbA_{1c} with different routes.

Method	Linear range	Detection limit	Reference
Capillary electrophoresis	—	10 ng/mL	[30]
Chromatography	—	1μg/mL	[31]
Thiophene-3-boronic acid monolayer covered gold electrode	0.1-1.0 μg/mL	—	[15]
Dendrimer/formylphenyl boronic acid modified electrode	2.5-15%	—	[32]
Poly(terthiophene benzoic acid)/gold nanoparticles modified electrode	0.1-1.5%	0.052%	[33]
Ferroceneboronic acid-based amperometric biosensor	6.8-14%	—	[29]
AuNPs/N-doped GNs/FTO	10-65 μg/mL	1.70 μg/mL	This work

Table 2. Interference result of determination of HbA_{1c} with other common species.

Interference species	Current change (%)	Interference species	Current change (%)
Hb	7.44	Glu	3.62
Fru	2.07	Gal	1.26

The current response to HbA_{1c} (50 μg/mL) in phosphate buffer solution (PBS) (0.1 M, pH 8.0) was measured to study the long-term stability, reproducibility and repeatability of the developed approach to HbA_{1c} determination. With respect to repeatability, the relative standard deviation (RSD) was obtained as 2.9% for 9 consecutive assays using DPV. Parallel experiments were performed using 6 electrodes with varied modification to evaluate the reproducibility (RSD, 7.4%). The proposed electrode retained ca. 97% of the initial voltammetric response after storage in a refrigerator at 4 °C, even as long as 1 month, suggesting the desirable long-term stability. A glycated hemoglobin A1c (GHbA1c) ELISA Kit (Cusabio) was used for comparison in a real sample (Table 3). As seen from the obtained recoveries, the fabricated immunosensor demonstrated outstanding accuracy for HbA_{1c} detection. Hence, the AuNPs/N-doped GNs/FTO was confirmed to be extremely stable.

Table 3. Recoveries of as-proposed sensor for the detection of HbA_{1c}.

Sample	Added (μg/mL)	Found (μg/mL)	Recovery (%)	RSD (%)	ELISA kit(μg/mL)
1	20	19.85	101	3.6	19.87
2	40	39.59	108	1.2	39.86

4. CONCLUSIONS

This study proposed the fabrication of AuNPs/GNs/FTO interface to achieve a sensitive electrochemical determination of HbA1c. A cross-linking technique was employed to immobilize FAO, providing higher stability to the working electrode. Therefore, the voltammetric sensor is highly selective and sensitive towards the determination of HbA_{1c}. In addition, the proposed sensor is low-cost and facile due to the accessibility of the determination reagents and simple filtration approach.

References

1. D. Goldstein, R. Little, R. Lorenz, J. Malone, D. Nathan, C. Peterson and . Sacks, *Diabetes Care*, 27 (2004) 1761.
2. J. Camargo and J. Gross, *Journal of Clinical Pathology*, 57 (2004) 346.
3. W. John, *Scandinavian Journal of Clinical and Laboratory Investigation*, 66 (2006) 1.
4. W. John, *Clinical Chemistry and Laboratory Medicine*, 41 (2003) 1199.
5. J. Jeppsson, U. Kobold, J. Barr, A. Finke, W. Hoelzel, T. Hoshino, K. Miedema, A. Mosca, P. Mauri and R. Paroni, *Clinical Chemistry and Laboratory Medicine*, 40 (2002) 78.
6. S. Eckerbom, Y. Bergqvist and J. Jeppsson, *Annals of Clinical Biochemistry*, 31 (1994) 355.
7. F. Frantzen, K. Grimsrud, D. Heggli, A. Faaren, T. LøVli and E. Sundrehagen, *Clinical Chemistry*, 43 (1997) 2390.
8. Z. Zhao, J. Basilio, S. Hanson, R. Little, A. Sumner and D. Sacks, *Clinica Chimica Acta*, 446 (2015) 54.
9. W. Yang, J. Yan, G. Springsteen, S. Deeter and B. Wang, *Bioorganic & Medicinal Chemistry Letters*, 13 (2003) 1019.
10. K. Kataoka, I. Hisamitsu, N. Sayama, T. Okano and Y. Sakurai, *Journal of Biochemistry*, 117 (1995) 1145.
11. B. Wang and J.-i. Anzai, *Materials*, 8 (2015) 1187.

12. Y. Zhou, H. Dong, L. Liu, Y. Hao, Z. Chang and M. Xu, *Biosensors and Bioelectronics*, 64 (2015) 442.
13. A. Chopra, S. Rawat, V. Bhalla and C. Suri, *Electroanalysis*, 26 (2014) 469.
14. D. Kim and Y. Shim, *Anal. Chem.*, 85 (2013) 6536.
15. J. Park, B. Chang, H. Nam and S.-M. Park, *Anal. Chem.*, 80 (2008) 8035.
16. J. Halámek, U. Wollenberger, W. Stöcklein and F. Scheller, *Electrochimica Acta*, 53 (2007) 1127.
17. N. Chauhan and C. Pundir, *Biosensors and Bioelectronics*, 61 (2014) 1.
18. T. Horiuchi, T. Kurokawa and N. Saito, *Agricultural and Biological Chemistry*, 53 (1989) 103.
19. L. Liu, S. Hood, Y. Wang, R. Bezverkov, C. Dou, A. Datta and C. Yuan, *Clinical Biochemistry*, 41 (2008) 576.
20. Y. Shao, J. Wang, H. Wu, J. Liu, I.A. Aksay and Y. Lin, *Electroanalysis*, 22 (2010) 1027.
21. G. Yang, Y. Li, R.K. Rana and J. Zhu, *Journal of Materials Chemistry A*, 1 (2013) 1754.
22. L. Sun, L. Wang, C. Tian, T. Tan, Y. Xie, K. Shi, M. Li and H. Fu, *Rsc Advances*, 2 (2012) 4498.
23. Y. Li, W. Gao, L. Ci, C. Wang and P. Ajayan, *Carbon*, 48 (2010) 1124.
24. P. Kannan, T. Maiyalagan, N. Sahoo and M. Opallo, *Journal of Materials Chemistry B*, 1 (2013) 4655.
25. Y. Zhang, G. Zeng, L. Tang, J. Chen, Y. Zhu, X. He and Y. He, *Anal. Chem.*, 87 (2015) 989.
26. M. Gholivand, N. Karimian and M. Torkashvand, *Journal of Analytical Chemistry*, 70 (2015) 384.
27. J. Liu, H. Tang, B. Zhang, X. Deng, F. Zhao, P. Zuo, B.C. Ye and Y. Li, *Anal Bioanal Chem*, 408 (2016) 4287.
28. N. Atar, M. Yola and T. Eren, *Appl. Surf. Sci.*, 362 (2016) 315.
29. S. Liu, U. Wollenberger, M. Katterle and F. Scheller, *Sensors and Actuators B: Chemical*, 113 (2006) 623.
30. M. Marinova, S. Altinier, A. Caldini, G. Passerini, G. Pizzagalli, M. Brogi, M. Zaninotto, F. Ceriotti and M. Plebani, *Clinica Chimica Acta*, 424 (2013) 207.
31. M. del Castillo Busto, M. Montes-Bayón, E. Añón and A. Sanz-Medel, *Journal of Analytical Atomic Spectrometry*, 23 (2008) 758.
32. Y. Han, S. Song and H. Yoon, *Journal of Bioscience and Bioengineering*, 108 (2009) S156.
33. Y. Zhu, J. Son and Y. Shim, *Biosensors and Bioelectronics*, 26 (2010) 1002.